Supporting Materials for

Self-photosensitized cycloaddition induced synthesis of high-density fuel with ultra-low freezing point using bulk bio-benzaldehyde and furans

Bo Yang[a,1], Jiawei Xie[b,1], Yuxuan Liang[a], Xiumei Ma[a], Huyao Ge[a], Xueping Wang[a], Zhaohui Wang[a,c], Qiuyu Zhang[a,*], Ji-Jun Zou[d], Junjian Xie[a,*]

[a] *School of Chemistry and Chemical Engineering, Northwestern Polytechnical University, Xi'an, 710072, China*

[b] *Institute of New Energy and Low-Carbon Technology, Sichuan University, Chengdu, 610065, China*

[c] *Department of Chemistry, Tsinghua University, Beijing, 100084, China*

[d] *School of Chemical Engineering and Technology, Tianjin University, Tianjin, 300072, China*

[1] *These authors contributed equally.*

[*] *Corresponding author. E-mail: qyzhang@nwpu.edu.cn, xiejunjian@nwpu.edu.cn*

Figure S1 Mass spectrum of 2-MF trimer.

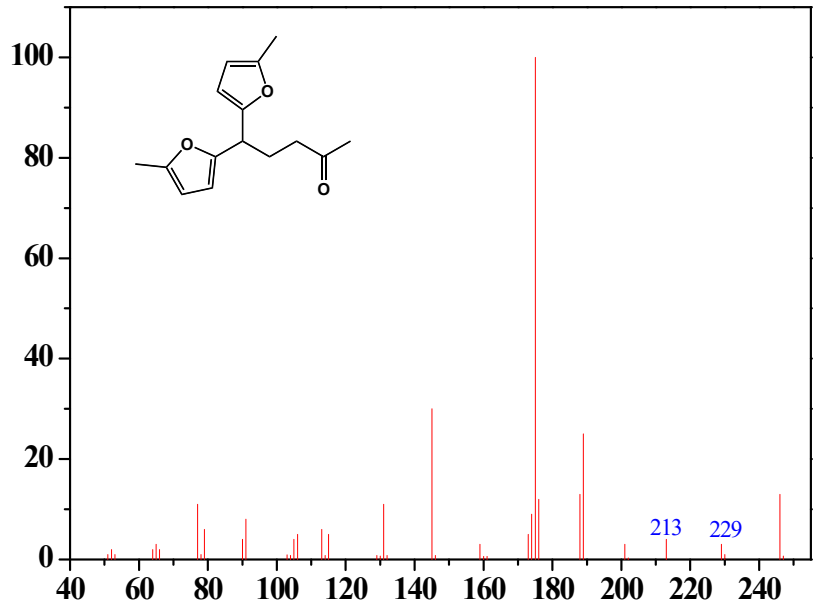

Figure S2 Mass spectrum of benzoin byproduct.

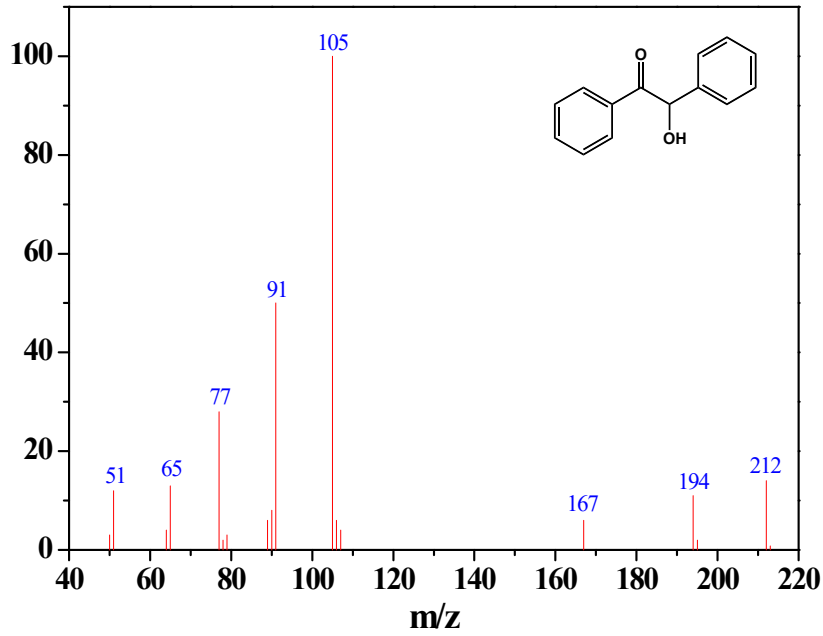

Figure S3 GC spectrum for the photoreaction of benzaldehyde and 2-MF.

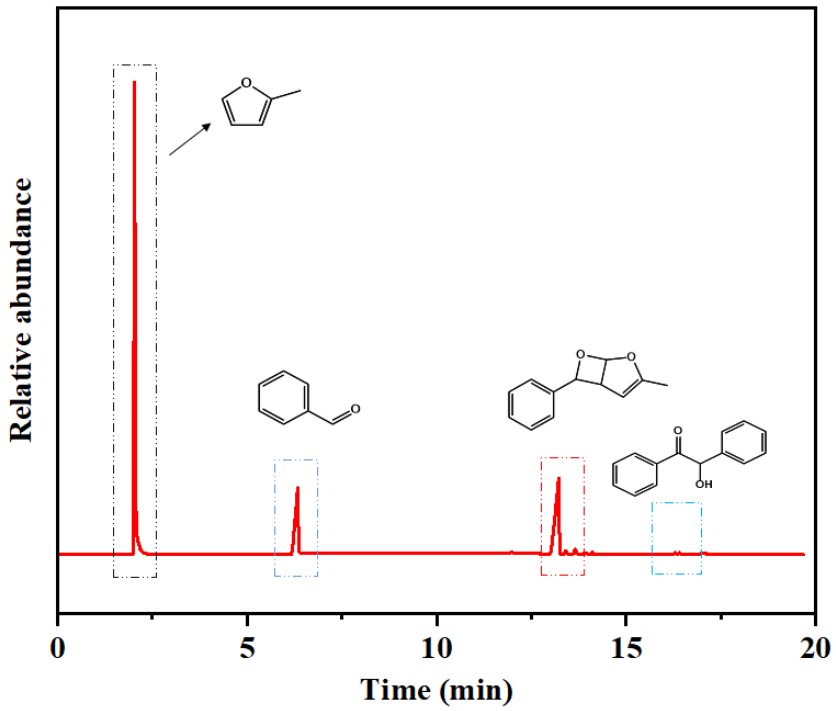

Figure S4 Mass spectrum for the cycloadduct of benzaldehyde/2-MF.

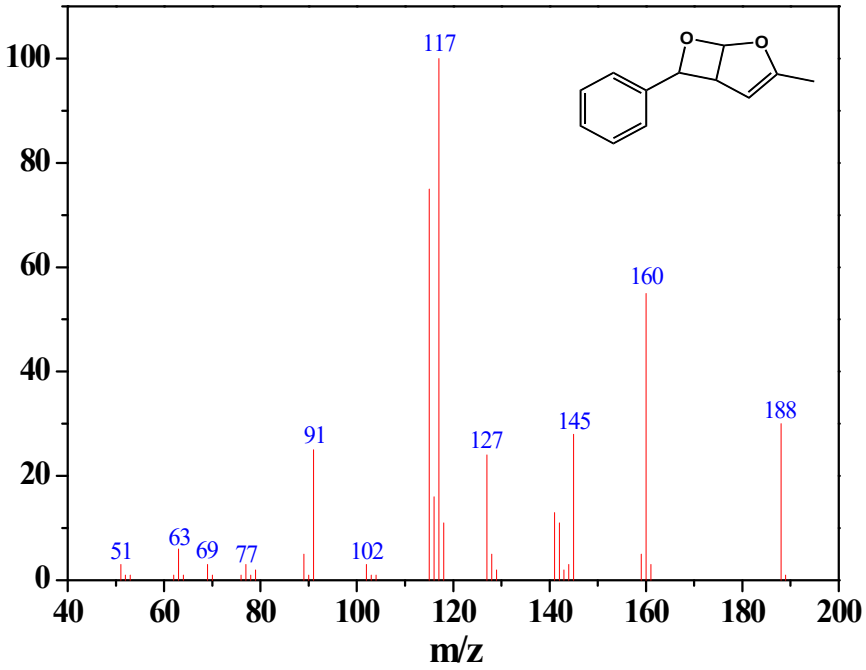

Figure S5 ^{1}H and ^{13}C NMR spectra for the cycloadduct of benzaldehyde/2-MF.

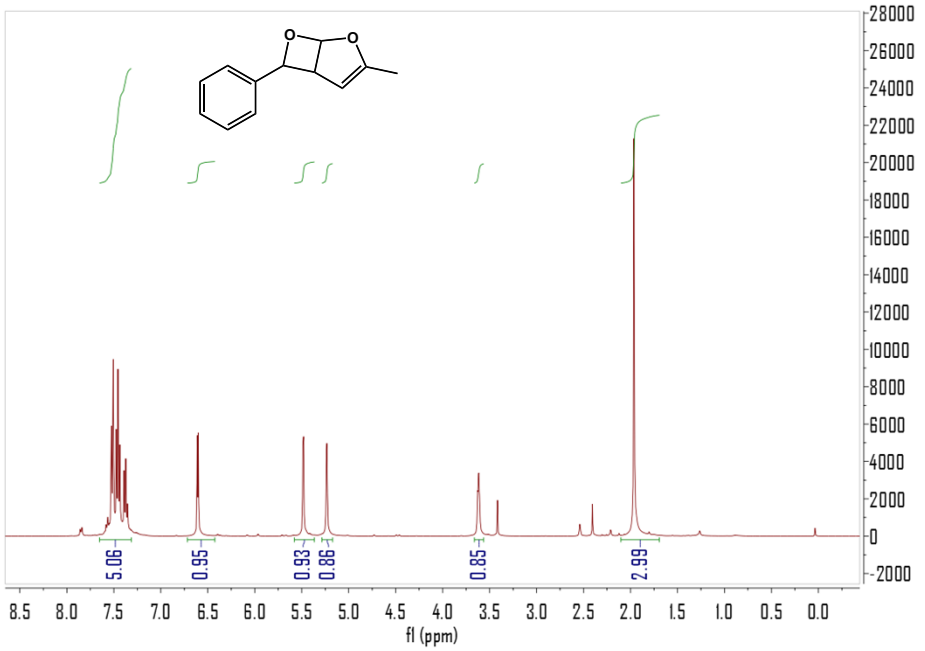

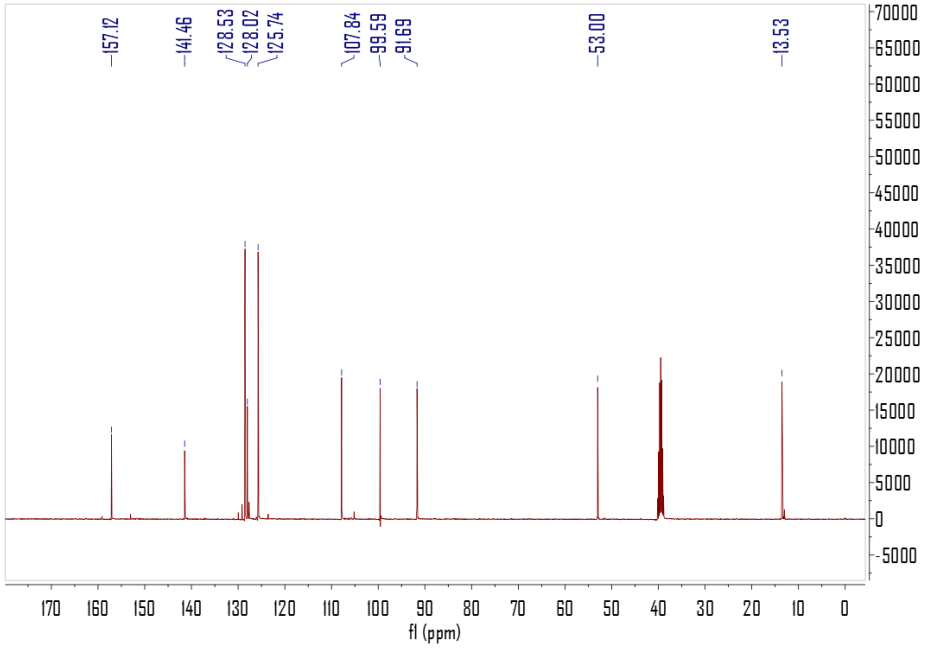

Figure S6 DEPT 90° ^{13}C NMR spectra for the cycloadduct of benzaldehyde/2-MF.

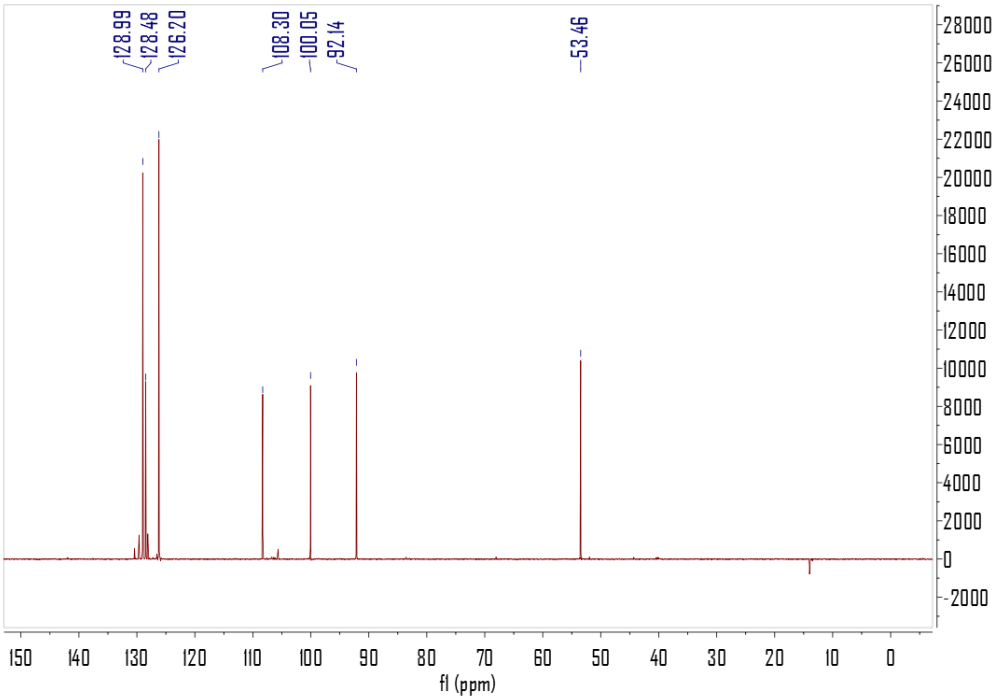

Figure S7 DEPT 135° ^{13}C NMR spectra for the cycloadduct of benzaldehyde/2-MF.

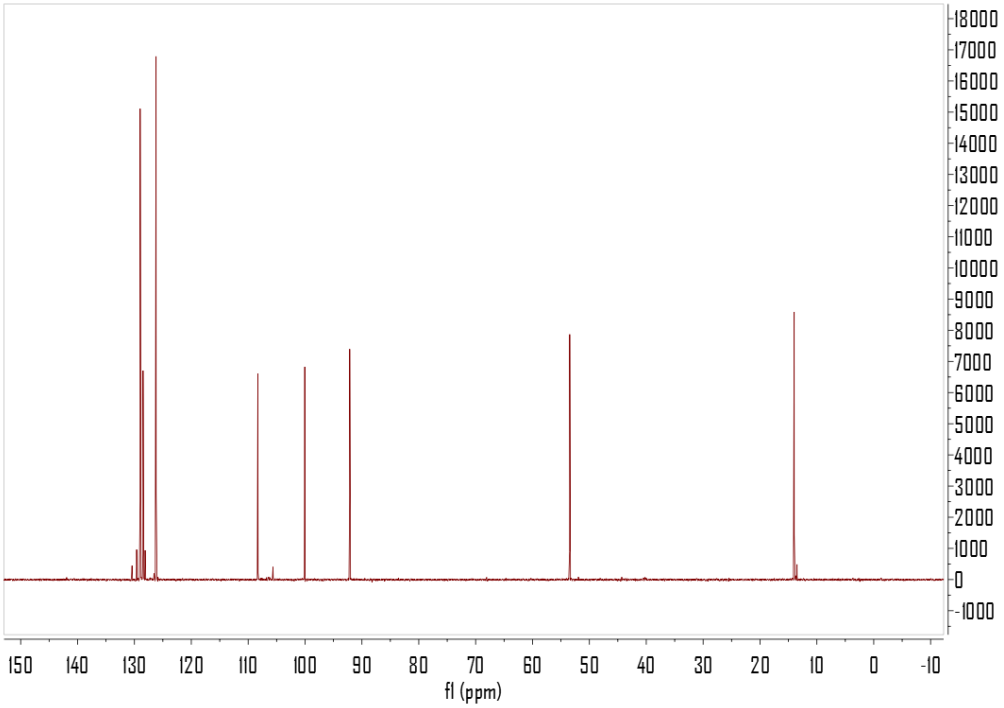

Figure S8 Mass spectrum for the cycloadduct of benzaldehyde and furan.

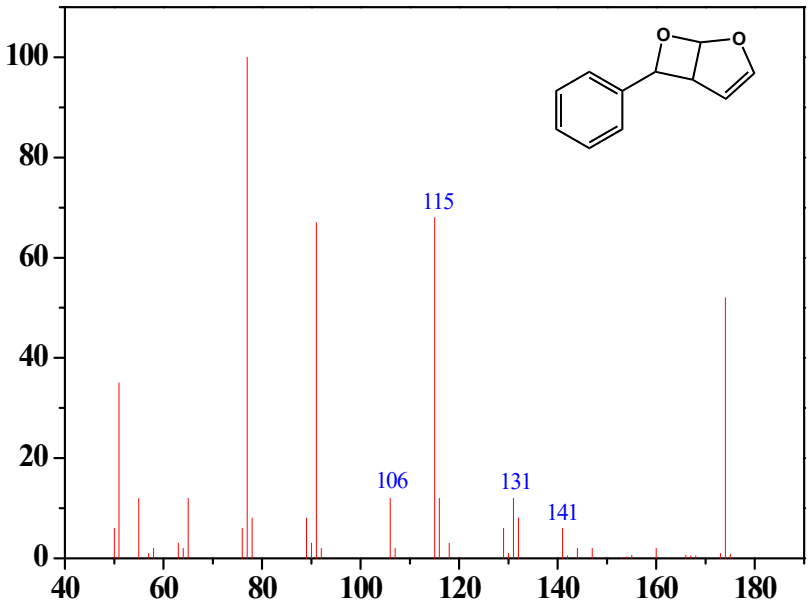

Figure S9 ^{1}H and ^{13}C NMR spectra for the cycloadduct of benzaldehyde/furan.

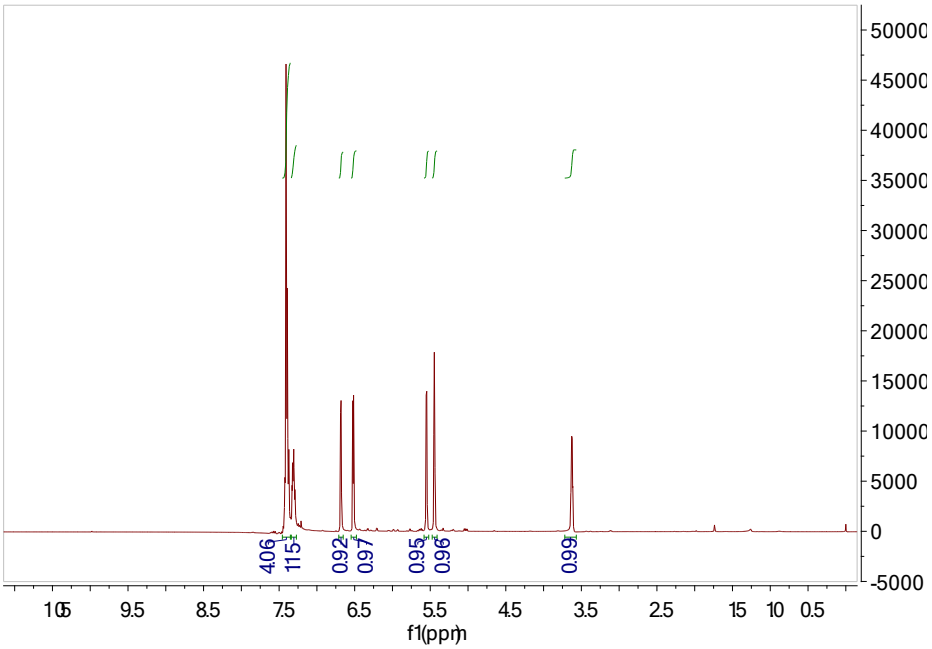

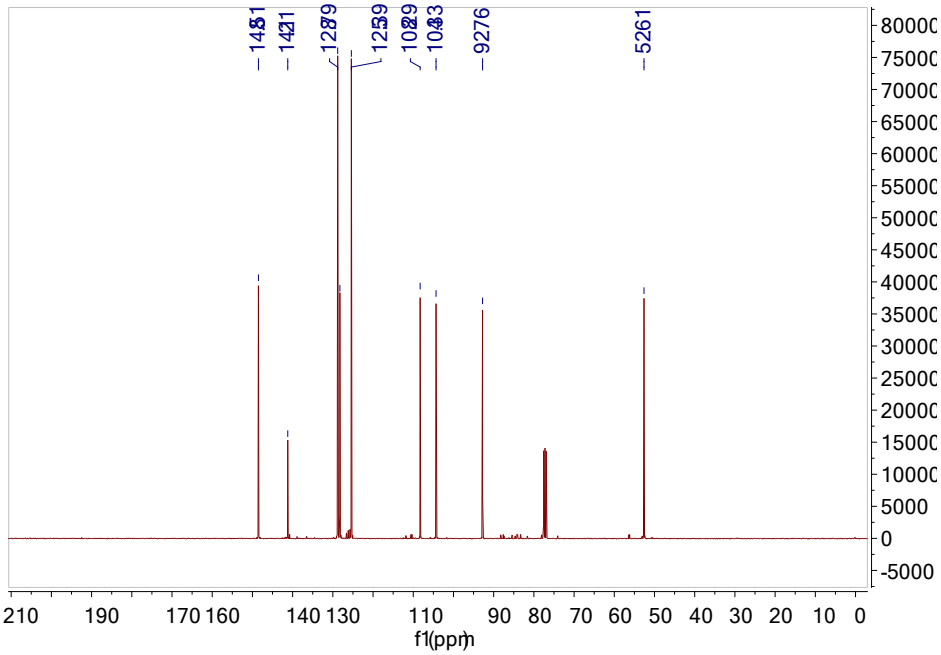

Figure S10 DEPT 45° ^{13}C NMR spectra for the cycloadduct of benzaldehyde/furan.

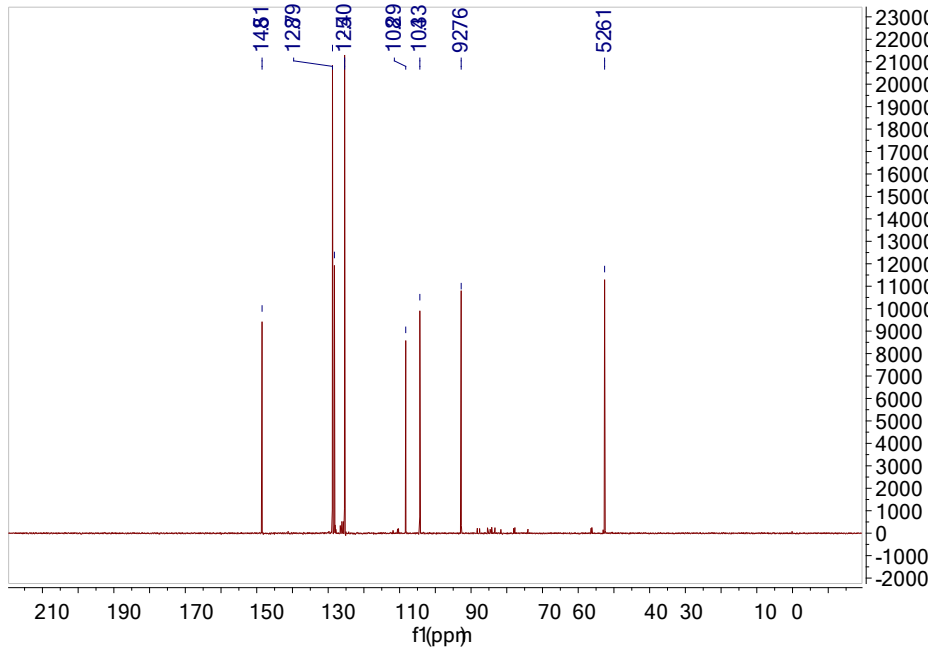

Figure S11 DEPT 90° ^{13}C NMR spectra for the cycloadduct of benzaldehyde/furan.

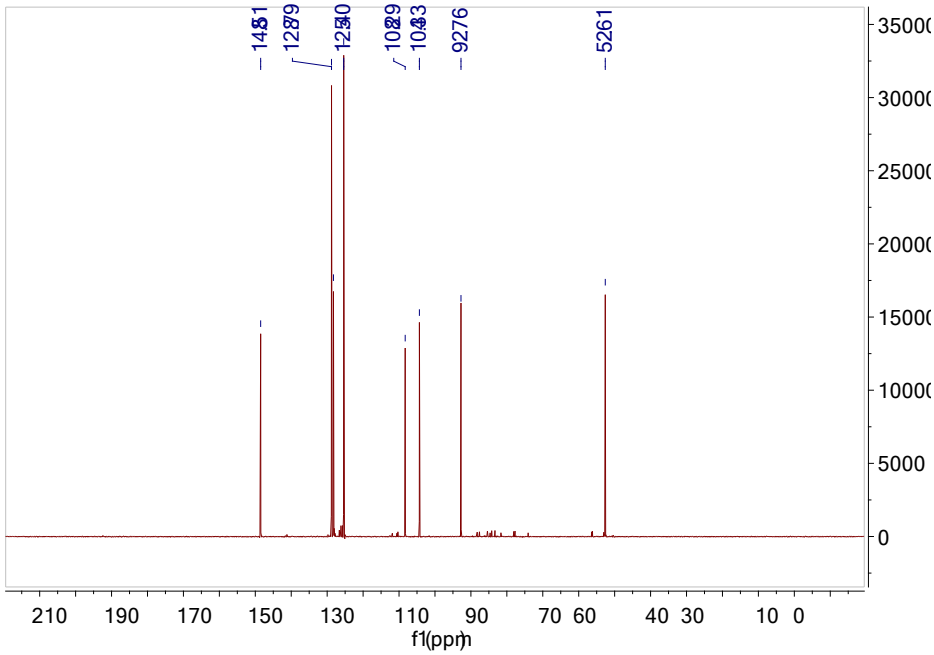

Figure S12 DEPT 135° ^{13}C NMR spectra for the cycloadduct of benzaldehyde/furan.

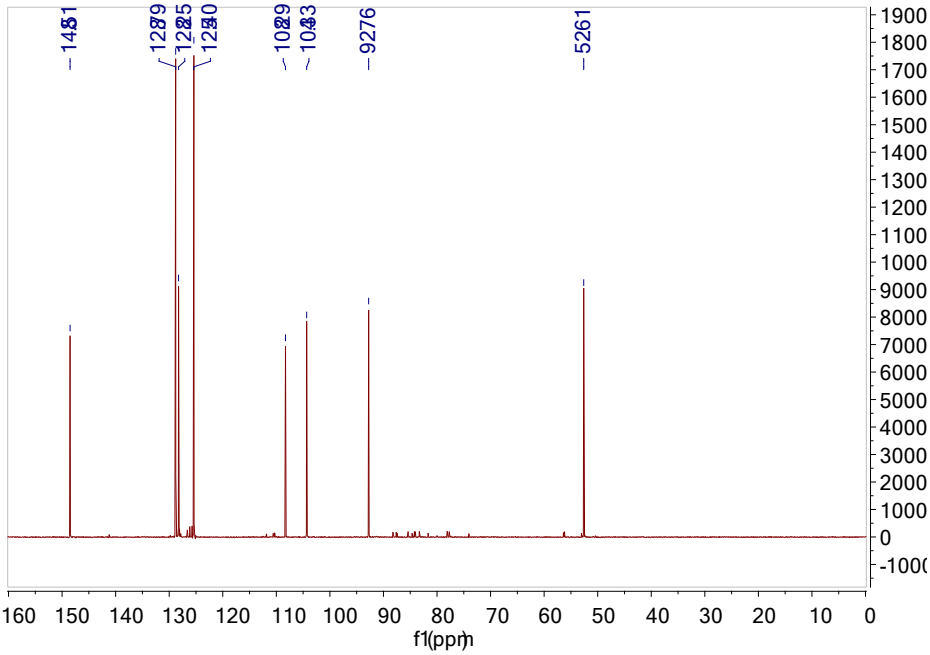

Figure S13 Mass spectrum for the cycloadduct of benzaldehyde and 2,5-dimethylfuran.

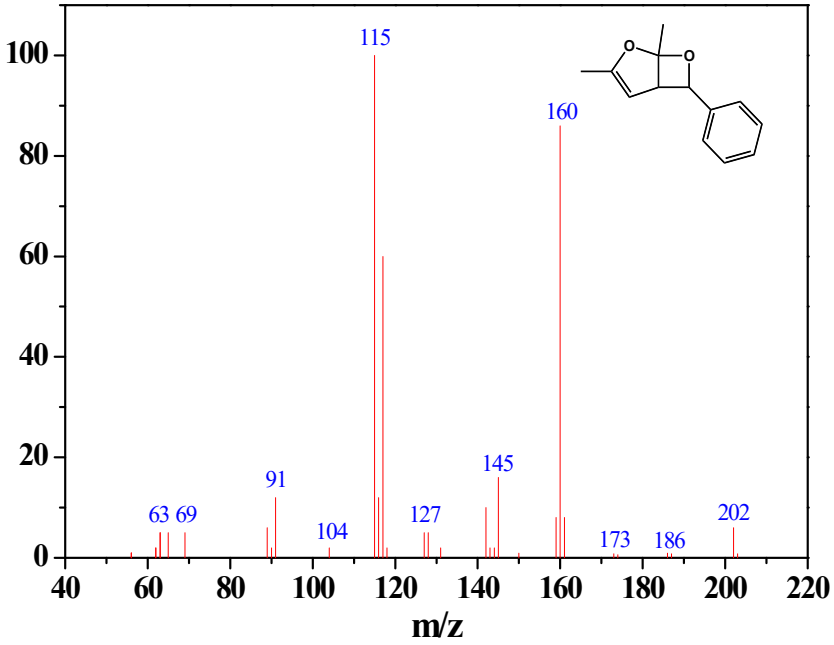

Figure S14 Mass spectrum for the cycloadduct of 4-methylbenzaldehyde and furan.

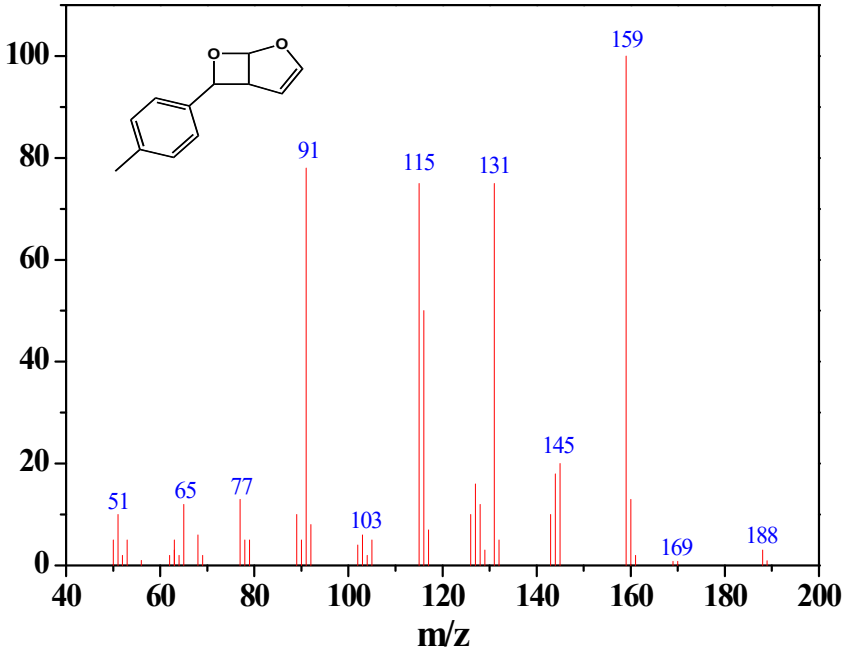

Figure S15 ^{1}H and ^{13}C NMR spectra for the cycloadduct of 4-methylbenzaldehyde and furan

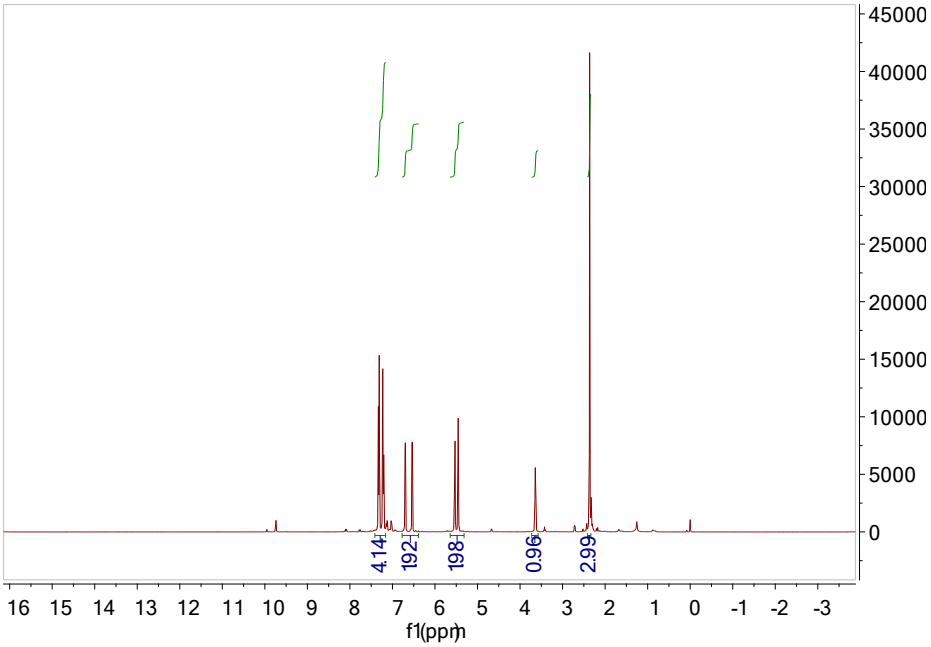

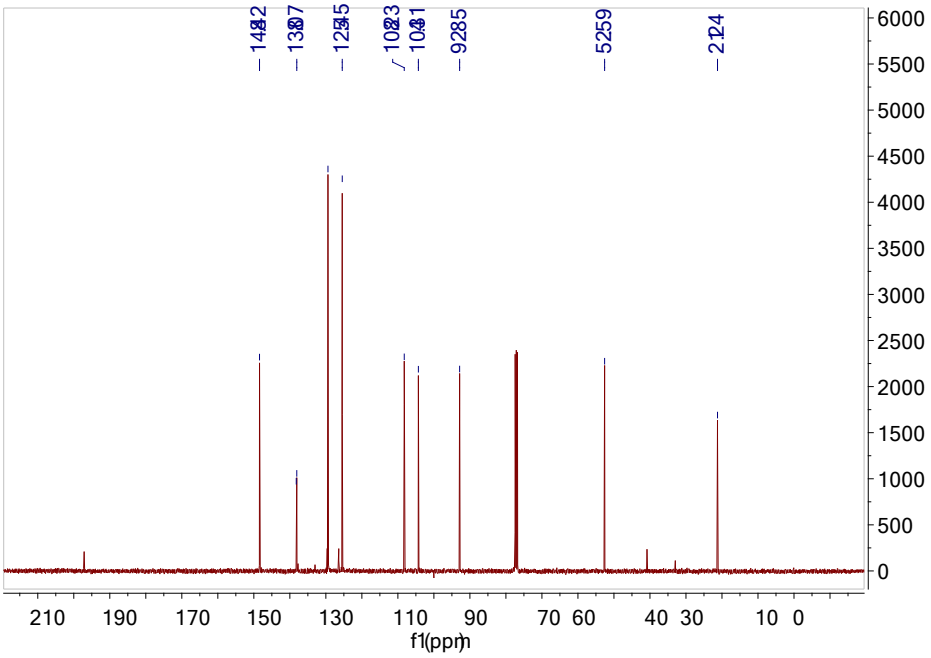

Figure S16 DEPT 45° ^{13}C NMR spectra for the cycloadduct of 4-methylbenzaldehyde and furan.

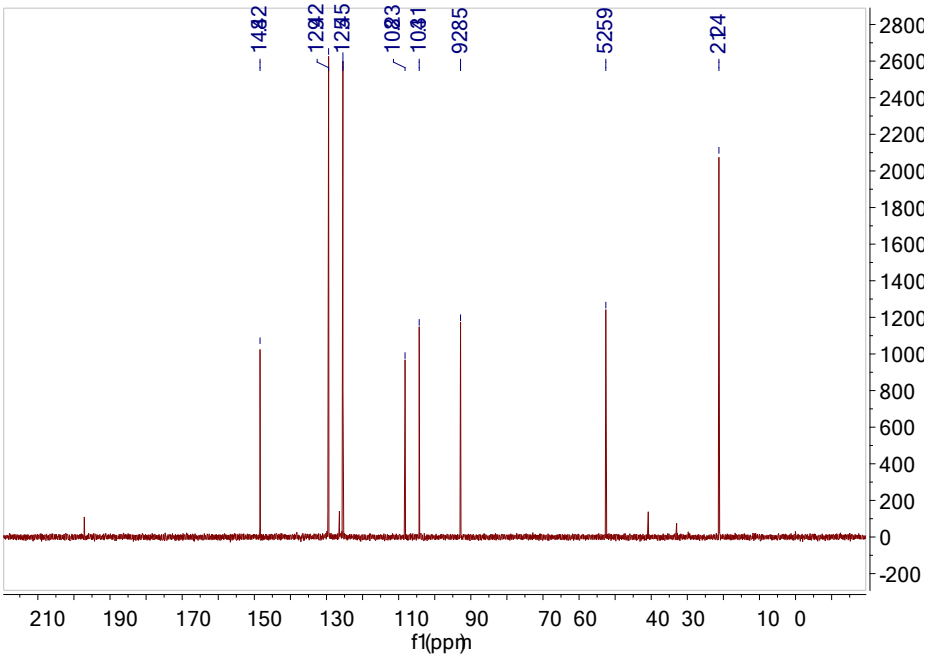

Figure S17 DEPT 90° ^{13}C NMR spectra for the cycloadduct of 4-methylbenzaldehyde and furan.

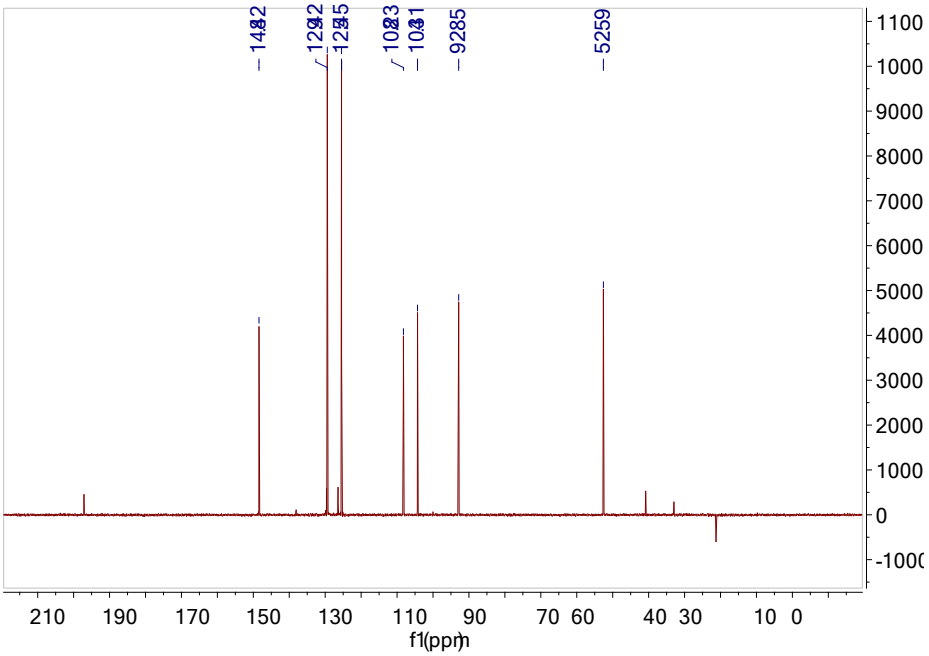

Figure S18 DEPT 135° ^{13}C NMR spectra for the cycloadduct of 4-methylbenzaldehyde and furan.

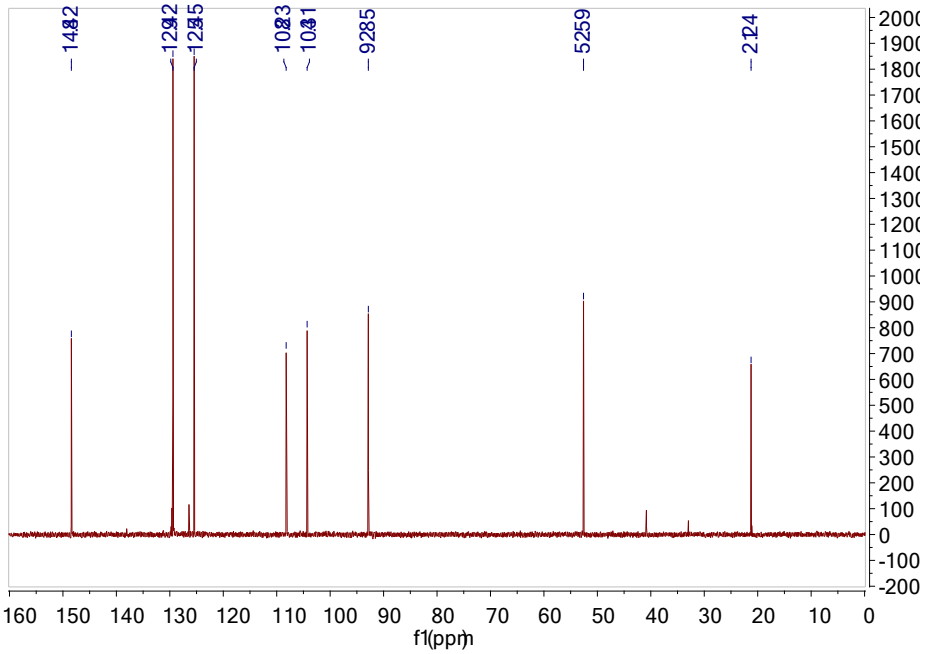

Figure S19 ^{1}H and ^{13}C NMR spectra for the cycloadduct of 4-chlorobenzaldehyde and furan

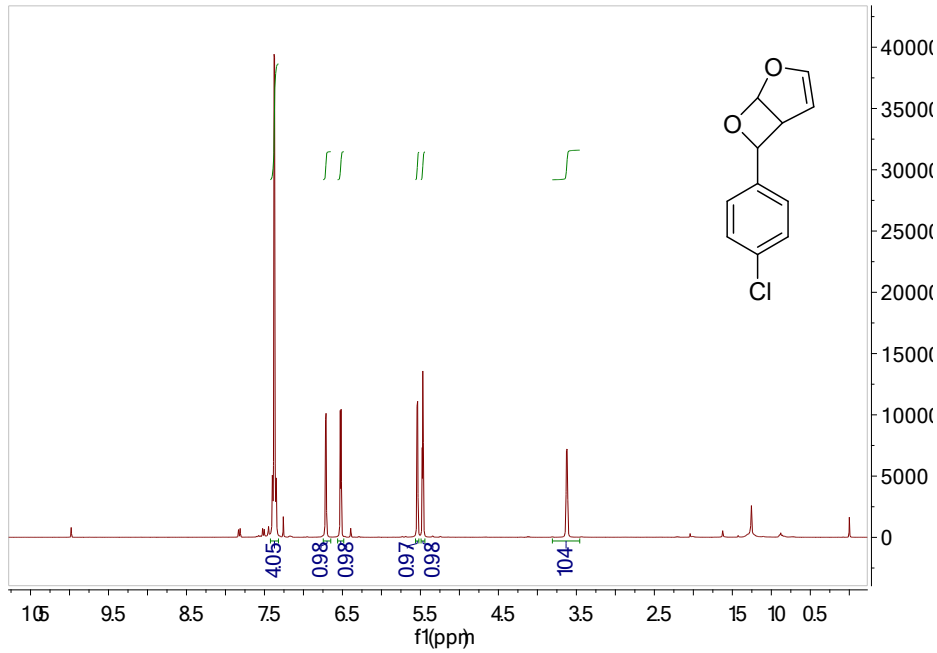

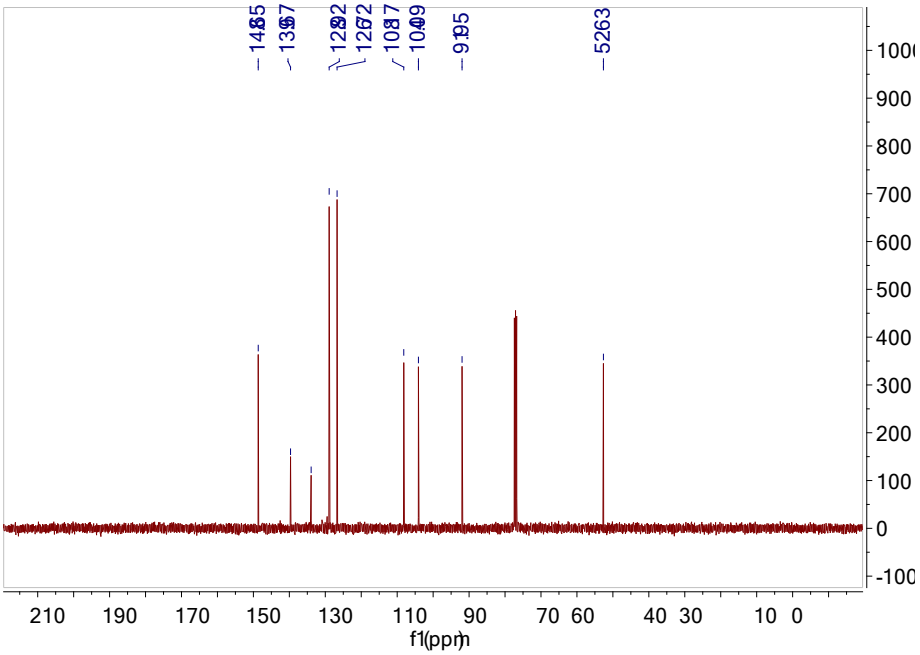

Figure S20 DEPT 45° ^{13}C NMR spectra for the cycloadduct of 4-chlorobenzaldehyde and furan

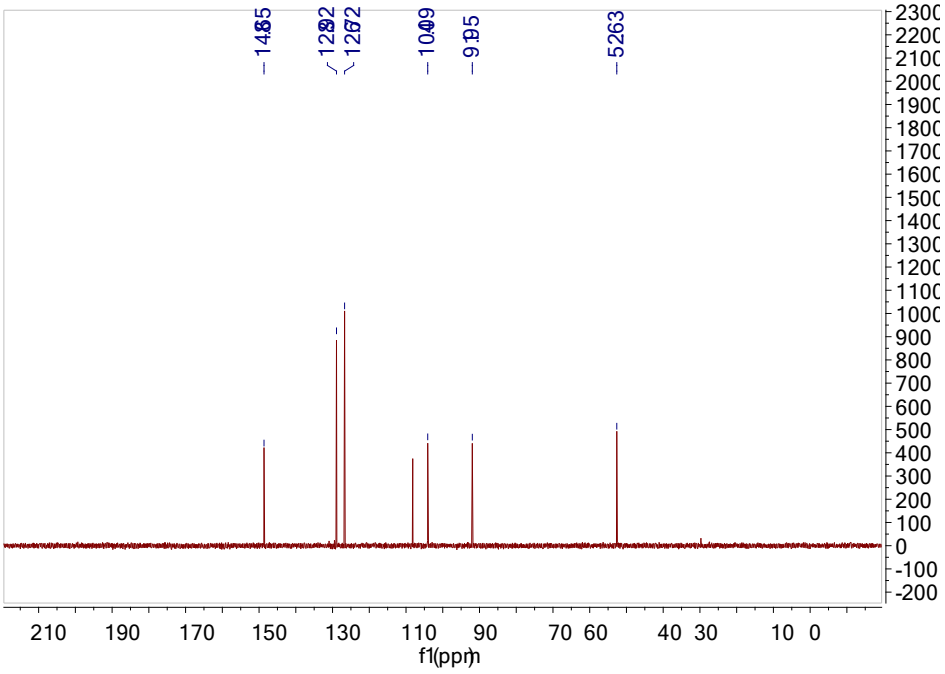

Figure S21 DEPT 90° ^{13}C NMR spectra for the cycloadduct of 4-chlorobenzaldehyde and furan

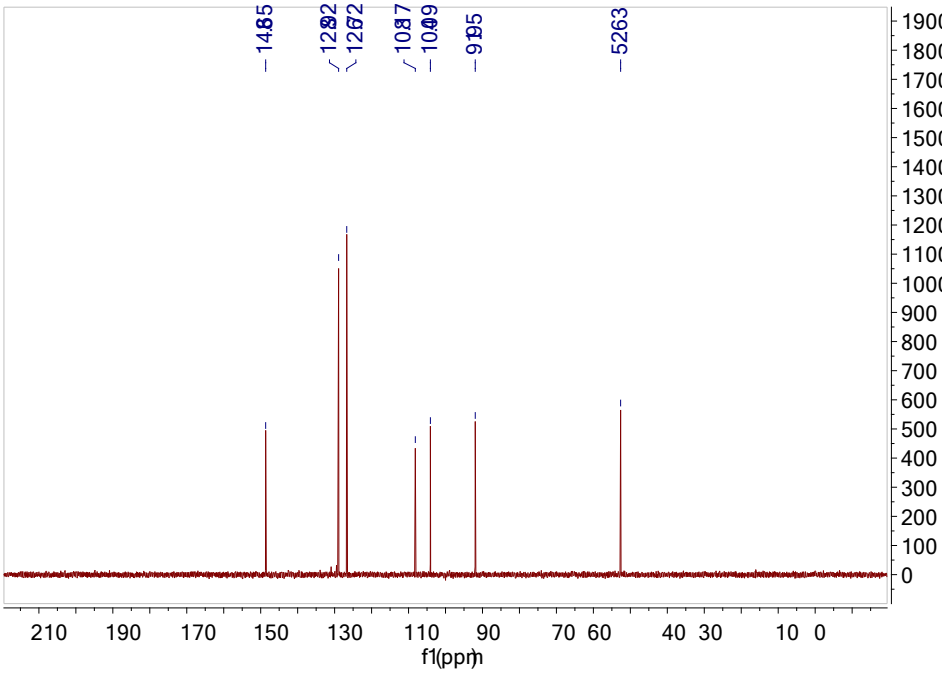

Figure S22 DEPT 135° ^{13}C NMR spectra for the cycloadduct of 4-chlorobenzaldehyde and furan

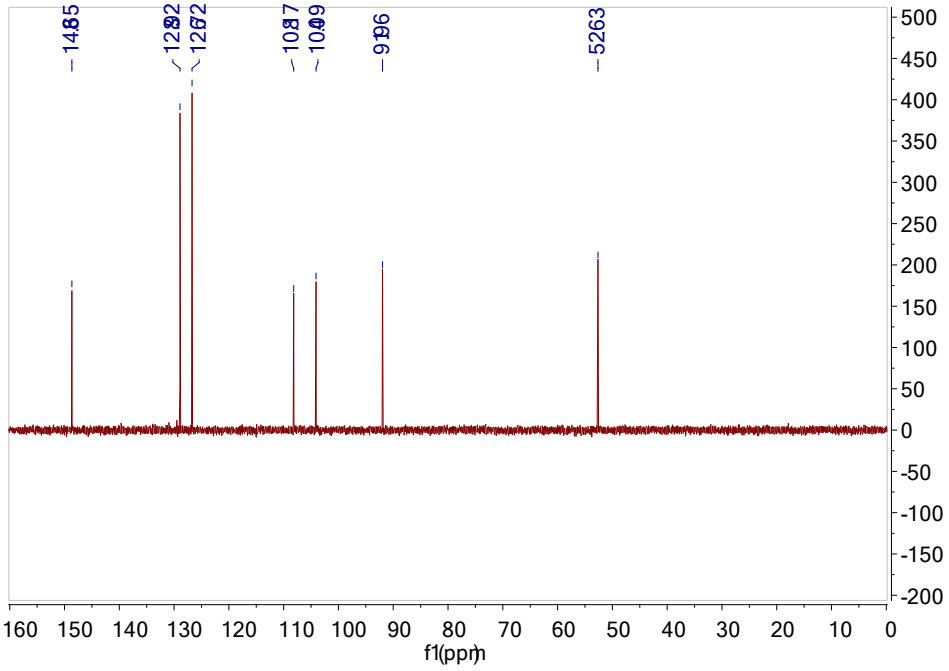

Figure S23 Mass spectrum for the cycloadduct of 4-methylbenzaldehyde and 2-MF.

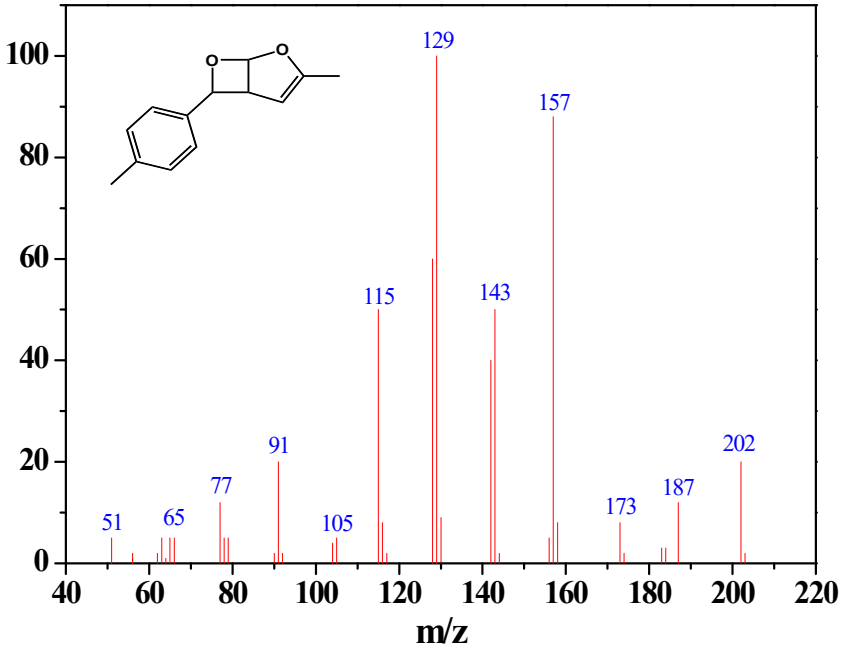

Figure S24 Mass spectrum for the cycloadduct of benzaldehyde and n-hexene.

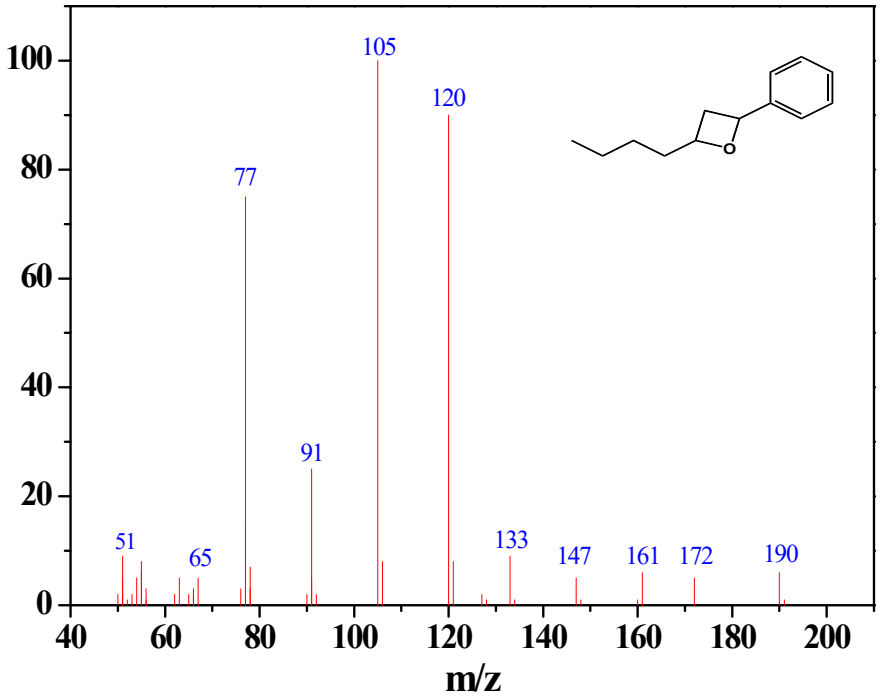

Figure S25 ^{1}H spectra for the cycloadduct of benzaldehyde and n-hexene.

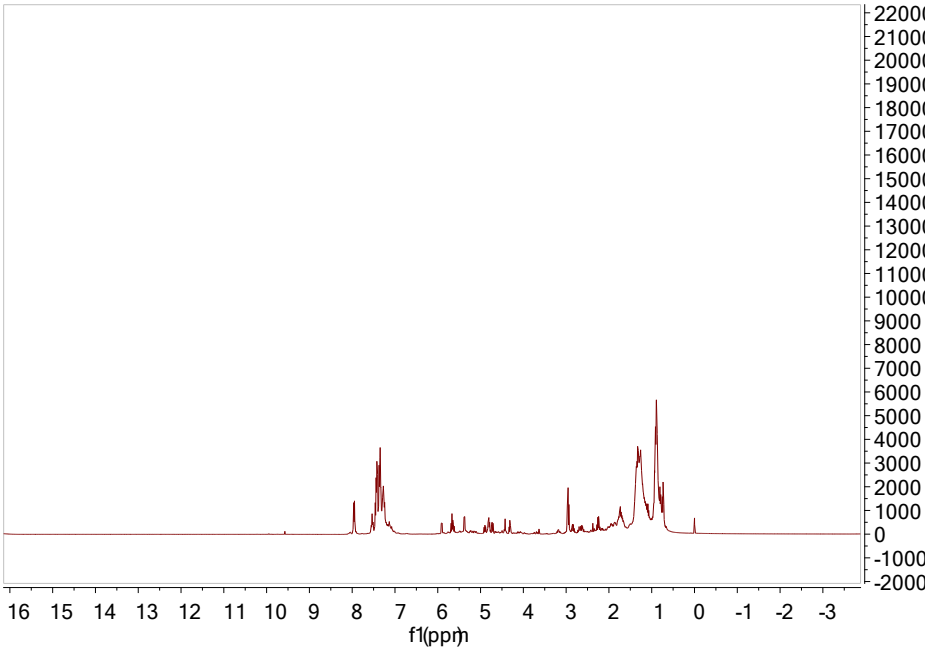

Attention: For reactants such as pinene and hexene, the inherent characteristics of their carbon skeletons may lead the radical intermediates to transform from the predicted configuration to a lower-energy radical state. Consequently, the resulting products comprise constitutional isomers with similar functional groups and structural features, rendering them inseparable by conventional column chromatography. These compounds are primarily characterized by ^{1}H NMR spectra, in which diagnostic signals corresponding to the hydrogen atoms of oxygen-containing rings, aromatic systems, and aliphatic groups can be observed. However, due to the coupling interactions among aliphatic hydrogens and the difficulty in purifying and separating structurally analogous products, further detailed analysis remains challenging.

Figure S26 Mass spectrum for the cycloadduct of benzaldehyde and cyclohexene.

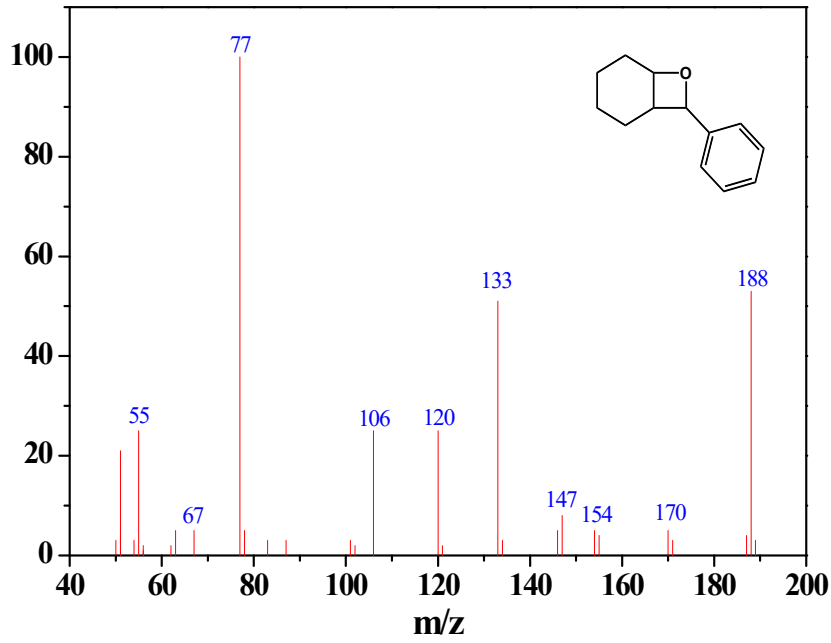

Figure S27 ^{1}H and ^{13}C NMR spectra for the cycloadduct of benzaldehyde and cyclohexene

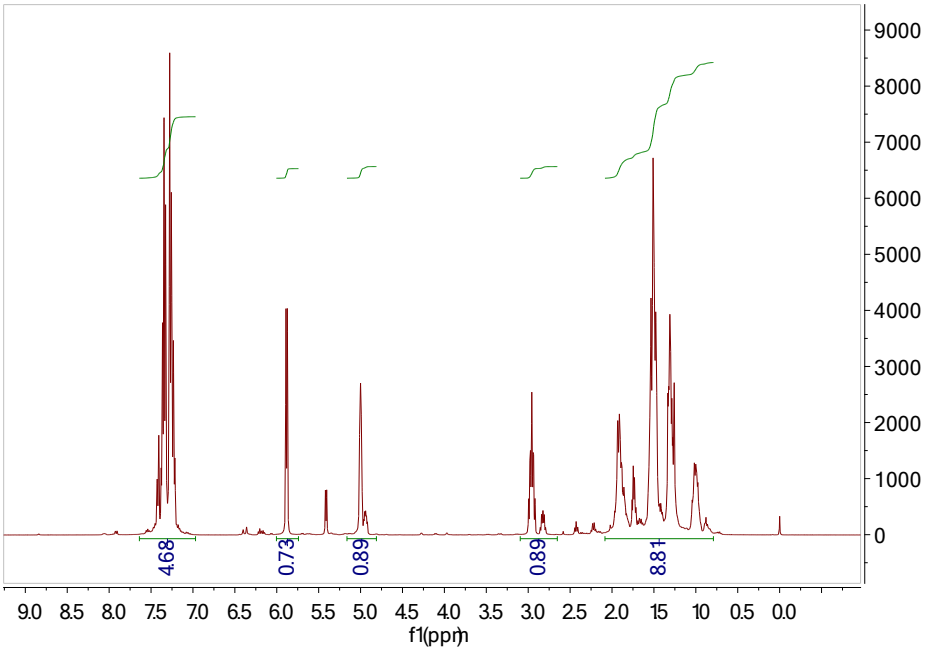

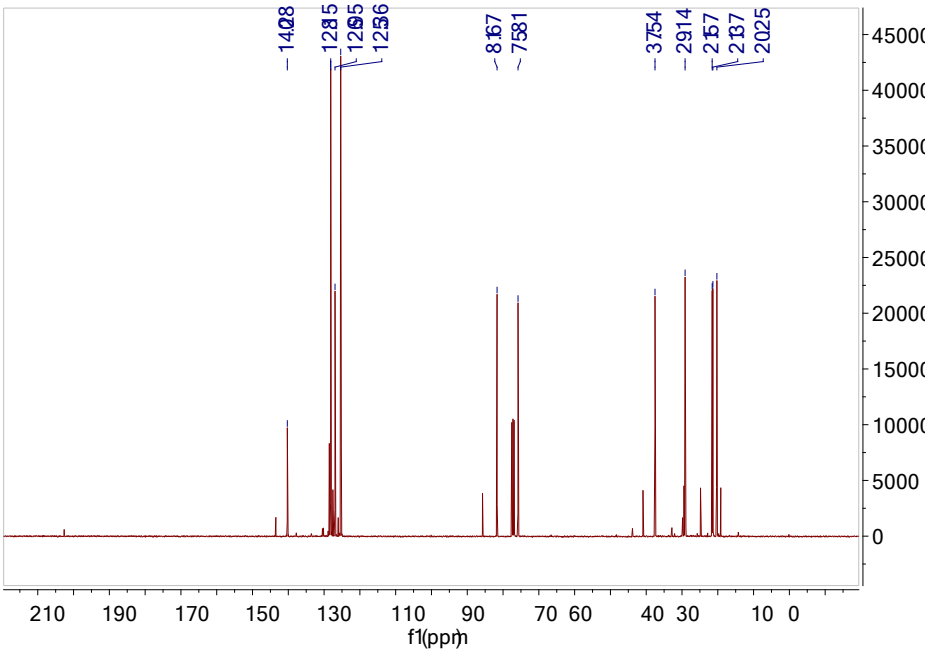

Figure S28 DEPT 45° ^{13}C NMR spectra for the cycloadduct of benzaldehyde and cyclohexene.

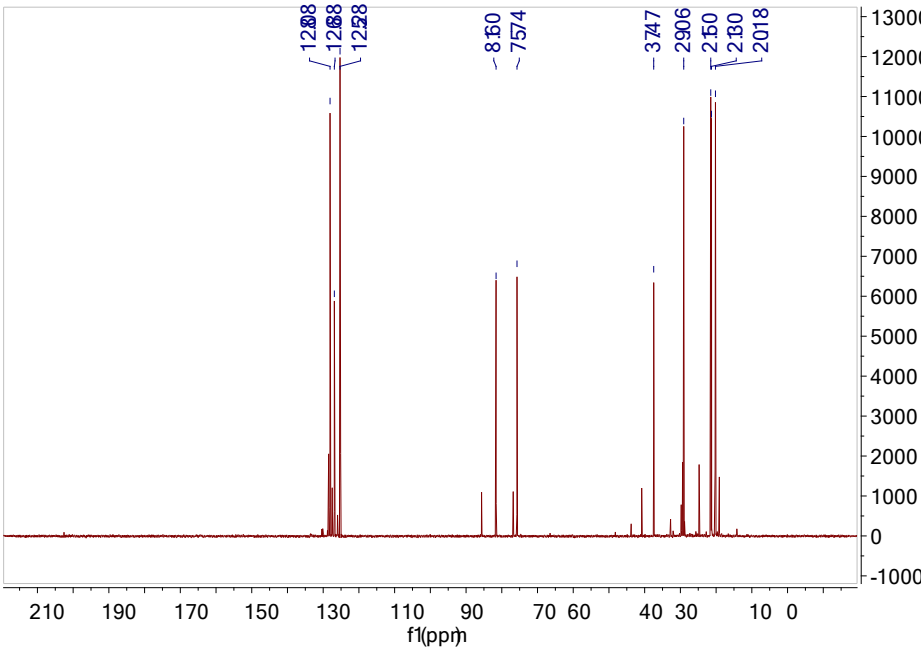

Figure S29 DEPT 90° ^{13}C NMR spectra for the cycloadduct of benzaldehyde and cyclohexene.

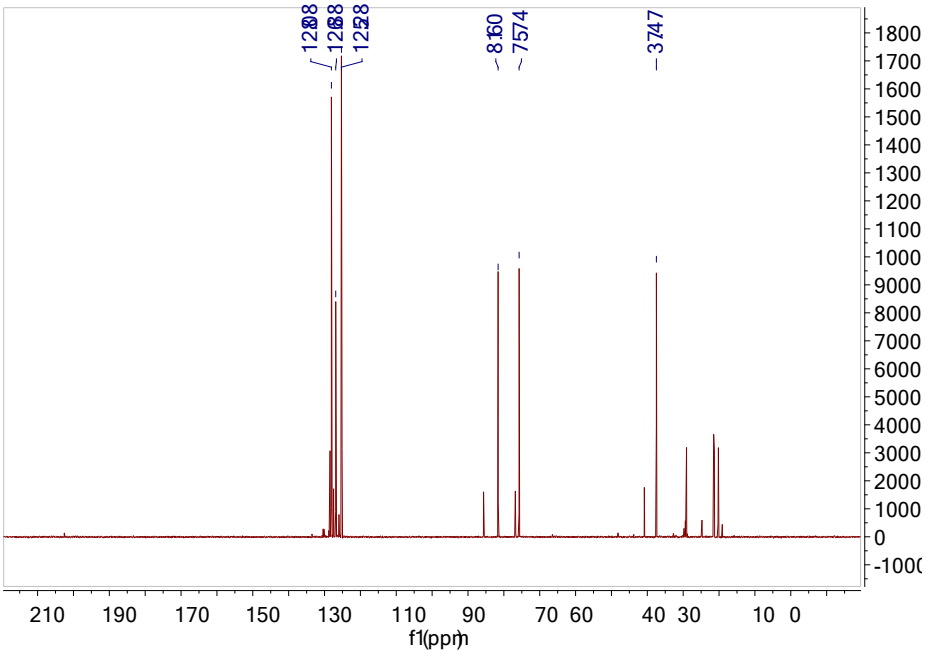

Figure S30 DEPT 135° ^{13}C NMR spectra for the cycloadduct of benzaldehyde and cyclohexene.

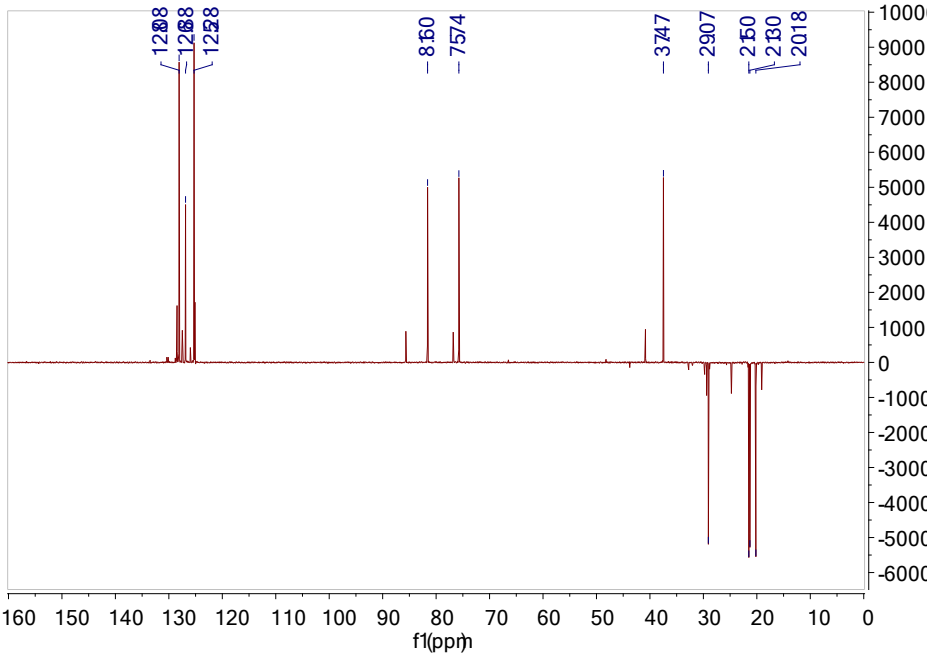

Figure S31 Mass spectrum for the cycloadduct of benzaldehyde and α-pinene.

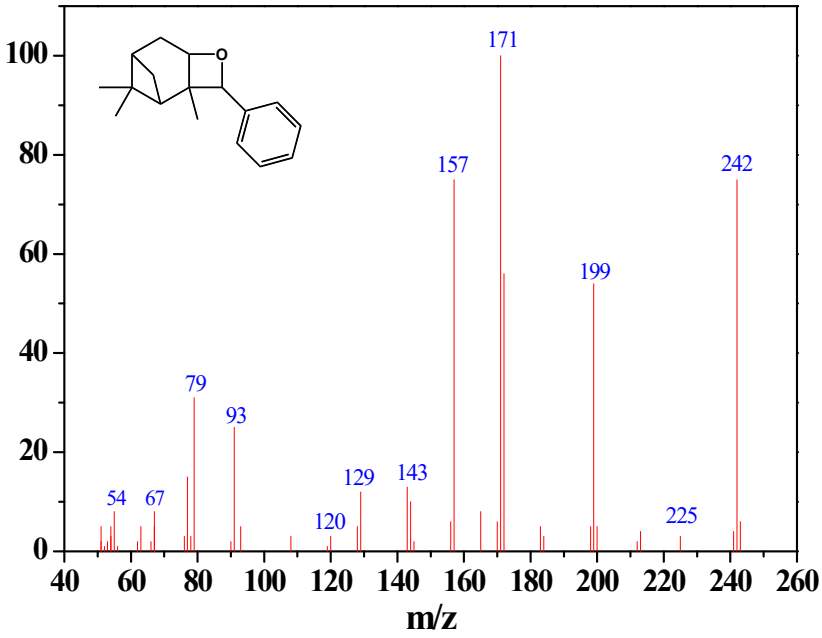

Figure S32 ^{1}H spectra for the cycloadduct of benzaldehyde and α-pinene

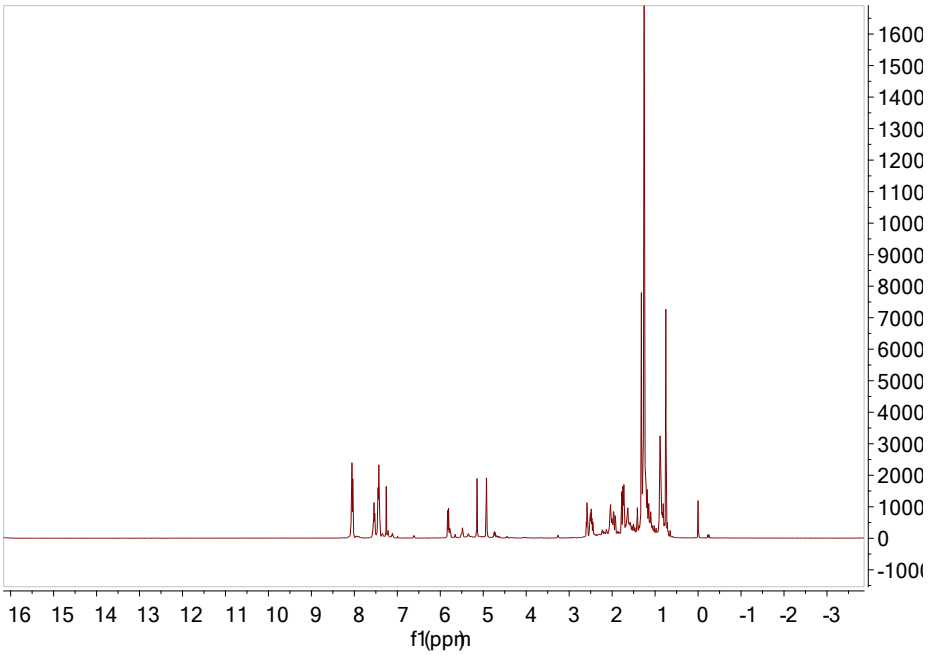

Figure S33 Mass spectrum for the cycloadduct of benzaldehyde and β-pinene.

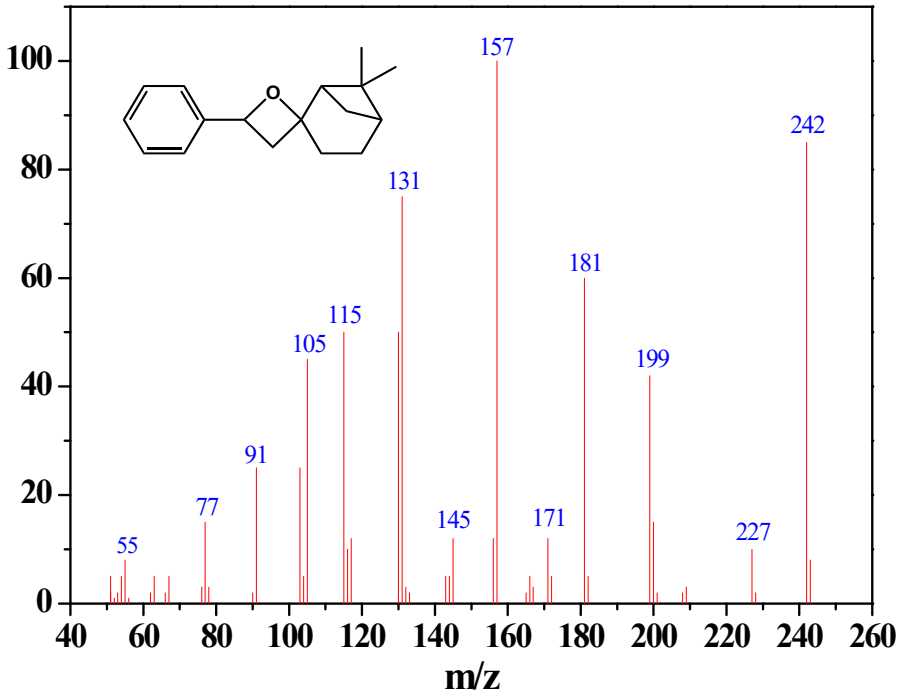

Figure S34 ^{1}H spectra for the cycloadduct of benzaldehyde and β-pinene

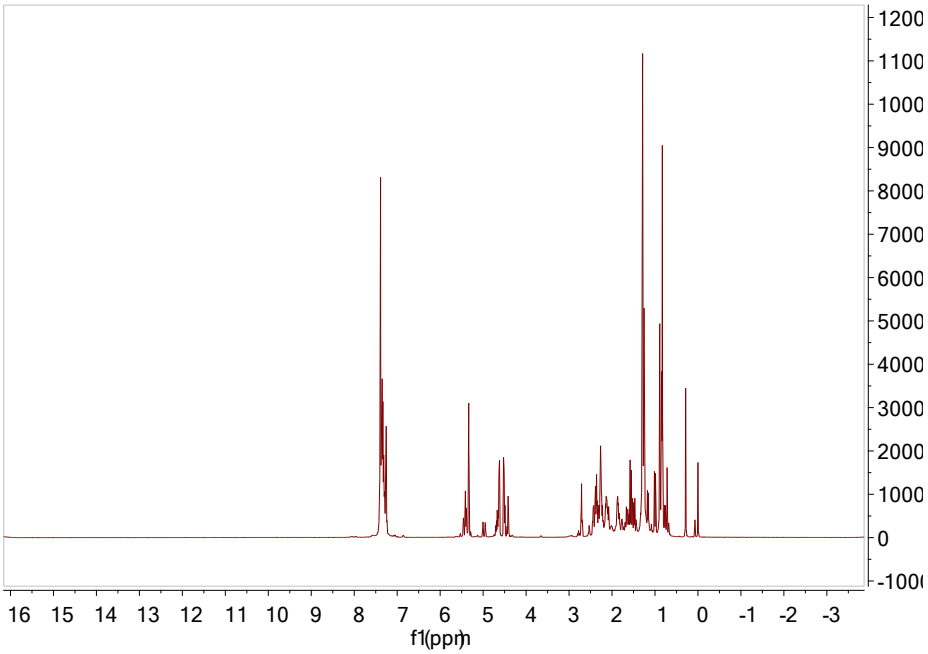

Figure S35 Mass spectrum for the final fuel derived from benzaldehyde and 2-MF.